

Chapter 12

Evaluating Weather Factors and Material Response During Outdoor Exposure to Determine Accelerated Test Protocols for Predicting Service Life

R. Sam Williams,¹ Steven Lacher,¹ and Corey Halpin¹
and Christopher White²

¹USDA Forest Service, Forest Products Laboratory, Madison, WI

²National Institute of Standards and Technology, Gaithersburg, MD

To develop service life prediction methods for the study of sealants, a fully instrumented weather station was installed at an outdoor test site near Madison, WI. Temperature, relative humidity, rainfall, ultraviolet (UV) radiation at 18 wavelengths, and wind speed and direction are being continuously measured and stored. The weather data can be integrated over time to calculate the dose of the weathering factors. In the study reported here, sealant test specimens were installed in a specially designed apparatus that subjected them to weather-induced cyclic movement that forced a response. Load-deflection information and weather were correlated to yield information on critical factors affecting the sealant performance. The results showed a clear link between the sealant response during weathering and the weather conditions causing this response. Instrumentation of the outdoor test facility and the data collection system are briefly described and methods for analyzing data are evaluated.

INTRODUCTION

As part of ongoing work at the USDA Forest Service: Forest Products Laboratory in Madison, WI, on the performance of materials used in residential construction, a study of sealants was begun in cooperation with the National Institute of Standards and Technology (NIST) (Gaithersburg, MD). This work involves detailed laboratory and field studies designed to develop service life prediction methods for sealants. A critical part of this work is the measurement of load and deflection of specimens as they are fatigue cycled during outdoor exposure. By measuring sealant load/deflection as the specimens are fatigue tested and the dose of various weather parameters that causes change in the load/deflection response, the degradation of specimens can be expressed in terms of weather “dose” rather than exposure time. The

This article was written and prepared by U.S. Government employees on official time, and it is therefore in the public domain and not subject to copyright. The use of trade or firm names in this publication is for reader information and does not imply endorsement by the U.S. Department of Agriculture of any product or service.

dose-response of the material obtained from outdoor testing accomplishes several advances over traditional time-response experiments. The most critical factors causing degradation can be established, interactions among factors can be determined, and dose-response from outdoor experiments can be compared with dose-response from accelerated laboratory experiments to obtain a meaningful acceleration factor.

General guidelines for accelerated testing of sealants are described by ASTM C 1142, Standard Practice for Conducting Tests on Sealants using Artificial Weathering Apparatus.1 Other ASTM methods for accelerated weathering of sealants are C 718-93 (UV-Cold Box Exposure of one-Part, Elastomeric, Solvent-Release Type Sealants), C 732-95 (Aging Effects of Artificial Weathering on Latex Sealants), C 734-93 (Low-Temperature Flexibility of Latex Sealants After Artificial Weathering), C 793-97 (Effects of Accelerated Weathering on Elastomeric Joint Sealants), C 1257 (Accelerated Weathering of Solvent-Release-Type Sealants), and D 2249 (Predicting Effect of Weathering on Face Glazing and Bedding Compounds on Metal Sash).¹ These tests use a weathering device with UV radiation and intermittent water spray to accelerate degradation. The tests are not meant to predict the exact service life nor the mechanism of failures, but are more of a qualitative evaluation of sealant performance. A sealant test that combines cyclic stress (fatigue), water immersion, and temperature change was initially developed by Hockman at NIST (ASTM C 719-93, Adhesion and Cohesion of Elastomeric Joint Sealants Under Cyclic Movement¹; the so-called Hockman cycle). Specimens are rated visually for cohesive or adhesive failure. Studies on the correlation of long-term artificial aging and outdoor exposure of sealants that focused on the degradation of cohesive properties and surface appearance were reviewed by Wolf.²

Several devices have been previously used to induce cyclic movement (fatigue) of sealants during exposure. These devices have generally used thermally induced dimensional change to generate fatigue. For example, Onuoha³ used unplasticized polyvinyl chloride (PVC) pipe to produce fatigue in one-part polyurethane and polyurethane-hybrid sealants. Racks have also been built using dissimilar materials such as wood and aluminum,⁴ concrete and aluminum,⁵ and steel and aluminum⁶ to develop fatigue stresses. Manually operated devices have also been used to create cycling effects.⁷

Sealants used in conjunction with glass, metals, and masonry are subjected to compression as these materials expand because of an increase in temperature and they are placed in tension as these materials cool. When sealants are in contact with wood, a change in temperature has the opposite effect. An increase in temperature causes the relative humidity in the surrounding environment to drop and the wood shrinks, placing the sealant in tension. In addition, moisture content changes caused by water can cause extremely large changes in dimension. Cyclic movement of sealants on the exterior of residential structures is caused primarily by moisture changes in wood and wood-based components; therefore, wood was chosen to cause the cyclic movement for initial outdoor tests. In more recent tests, however, the specimens can be fatigue cycled either thermally or by moisture.

Our approach to the design of the test devices for outdoor testing is to use both thermally driven and moisture driven devices to fatigue the test specimens. Thermally induced fatigue is important for sealants used in conjunction with materials such as glass, metals, and plastics, and moisture induced fatigue is important for sealants used in conjunction with wood and wood-based materials. The initial phase of outdoor testing focused on moisture induced fatigue cycling, and test apparatuses were designed using wood blocks to induce the cyclic motion. This chapter describes the construction of test apparatuses, instrumentation of the outdoor test facility, and data collection system, and shows possible methods for analyzing the data. The results show a clear link between the materials response during weathering and the

weather conditions causing this response. We believe this technology is relevant to all types of materials research in which outdoor fatigue cycle tests are needed to predict performance of materials.

The overall objective of this study was to develop a protocol for predicting the service life of sealant formulations and to identify the fundamental mechanisms of early failure. This protocol included both accelerated and outdoor exposures and evaluated the validity of current accelerated experimental protocols. Within this overall objective, all outdoor weathering factors (temperature, UV radiation, relative humidity, wind velocity, and rainfall) and their amount (dose) were monitored, and the sealant degradation (materials response) was linked to the dose. All four major environmental stress components (temperature, relative humidity, UV radiation, and interrelated cyclical motion) were measured. In short, our objectives were to (1) gather real-time data of stress and strain of sealants during outdoor exposure, (2) gather real-time data on weather, including UV radiation, and (3) match sealant response to accumulated environmental stresses.

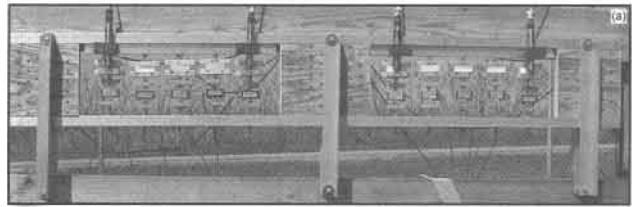
Ultimately our goal is to use the information from outdoor materials response and weather data to develop appropriate accelerated tests and the capability to determine service life in less than real time with statistical confidence and reasonable accuracy. All tests must be accurate and precise and laboratory tests must be repeatable.⁸

EXPERIMENTAL

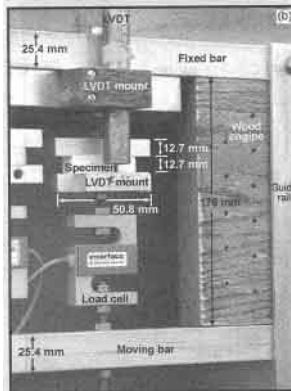
Equipment

TEST APPARATUS: The test apparatus subjects the specimens to movement in response to weather changes. The weather-induced movement of sealant specimens is obtained from the dimensional change in tangential blocks of red oak (*Quercus rubra*) as the wood wets and dries, from precipitation and/or changes in relative humidity. Because the movement of the wood causes the cyclic movement, it is referred to as the "wood engine"

Two designs (TS and CS) were developed for conducting these exposure tests. In TS (Figure 1), the test specimens are placed in tension (T) by an increase in moisture content of the wood [as the wood swells (S)]. This subjects the specimen to stresses similar to those obtained via

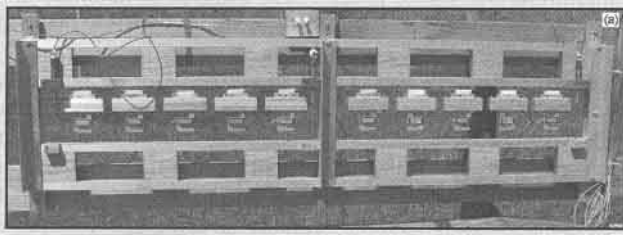


(a)



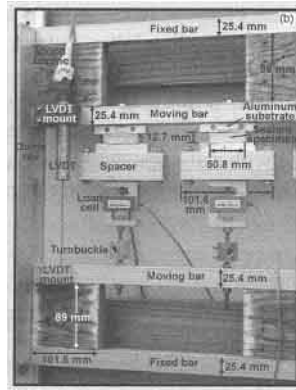
(b)

Figure 1-Designs TS: (a) apparatus places specimens in tension as wood swells; (b) details showing dimensions.



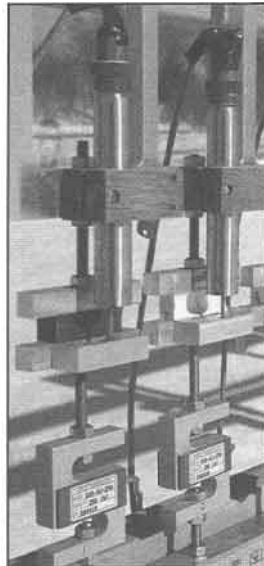
(a)

Figure 2-Design CS: (a) apparatus places specimens in compression as wood swells; (b) detail showing dimensions.



(b)

Figure 3-Sealant specimen, force transducer, and LVDT.



thermal expansion or contraction of metals, glass, ceramics, or polymers. This apparatus simulates the thermally driven designs previously used, but it is driven primarily by changes in relative humidity and water, not temperature. In CS (*Figure 2*), the test specimens are placed in compression (C) as the wood swells, which subjects the specimens to stresses similar to those obtained when sealants are used on wood.

The wood moves against an aluminum frame to produce a cyclic movement. The aluminum bar at the top is fixed, and the bar at the bottom is free to move. The load cell and specimen are uni-axial and are connected using a stainless steel threaded rod with locking nuts (*Figure 3*). All fasteners in the apparatus are stainless steel. Each specimen can be attached to a linear variable differential transformer (LVDT). However, we found that deflection could be determined using only four LVDTs. The apparatus is capable of giving a maximum deflection of about ± 3 mm. By adjusting the size of the wood and the aluminum, the maximum movement can be controlled. The LVDTs are sealed sensors (HSD-750, Macro Sensors, Pennsauken, NJ), with a deflection range of ± 6.35 mm. Force transducers (load cells) are used to measure the load in the system. The sealed transducers (Model SSM-AJ-250, Interface, Scottsdale, AZ) have a capacity of +113.4 kg.

Data Acquisition

Data from the force transducers and LVDTs were fed into a Keithley 2750 data acquisition system, using Keithley 7708 voltage measurement expansion cards (Keithley Instruments, Cleveland, OH). The field site and main laboratory are linked by computer. Data were collected using a custom program written in Lab View. This program periodically collects voltage measurements from the Keithley system, data from the UV radiation spectrometer (SR-18), and the weather instrumentation. The program then calculates force, deflection, stress, and strain based on the collected voltages. The result of the collection and calculation are called a "point." After 10 points have been collected, the program averages the values and appends the result to a tab-delimited data base.

The data collection rate varies depending on the rate of movement of the specimens. During periods of rapid movement, more data are collected. As movement slows, the rate of data collection slows. During periods of rapid movement, an average of the 10 measurements is recorded every 2.5 min. At the other extreme, an average of the 10 measurements is recorded every 25 min.

UV Radiometer

The UV measurements were made using a UV radiometer developed by the Smithsonian Environmental Research Center (SERC), Edgewater, MD. Personnel at SERC maintain the Calibration of the instrument, and this calibration is traceable to NIST standards. The instrument, designated as SR-18, is one of a network of similar instruments located at various sites within the United States. UV-radiation intensity is collected at the following wavelengths (in nanometers): 289.94, 291.30, 293.70, 295.93, 297.68, 299.70, 301.14, 303.75, 305.66, 307.47, 309.71, 312.22, 314.14, 315.76, 318.24, 319.96, 321.93, and 323.45. The radiometer is located on a tower 4 m above the ground; except for some trees located 200 m away, the view of the horizon is unobstructed in all directions.

Weather Station

The weather station has a modular design, which permits flexibility in terms of the type of sensors that can be used and the ability to modify the system to meet future needs. The pres-

ent configuration consists of an RM Young model 52202 wind meter, RM Young model 05103 tipping bucket rain gauge, and Paroscientific Met 3A weather station attached to a Campbell Scientific CR10X data-logger. The wind meter measures wind speed and direction. The rain gauge measures both rainfall and snowfall, using a built-in heating coil to melt snow. The weather station provides measurements of temperature, barometric pressure, and relative humidity with extremely high accuracy. This selection of instruments was recommended by SERC. Data are stored locally in a tab-delimited database as hourly averages; however, 1-min data are extracted for calculations.

MATERIALS

Wood

All wood engines were made from 25.4-mm (1-in.) thick flat sawn red oak (*Quercus rubra*). To enhance the rate of moisture content change, 3.2-mm ($\frac{1}{8}$ -in.) diameter holes were drilled through the oak blocks. The end grain was sealed to minimize checking. The oak block engines were installed in the test apparatus with the grain perpendicular to the strain direction so that the direction of maximum dimensional change was parallel to the specimen strain direction. For both sealant test apparatuses, total wood width was 178 mm (7 in.) in the strain direction (*Figures 1 and 2*).

Aluminum

Structural components of the apparatuses were made from aluminum because of its relatively high strength to weight ratio, and corrosion resistance. The frames were made from 6061-T6 aluminum. Sealant specimen substrates were made from 6063-T5 anodized aluminum.

Stainless Steel

Stainless steel hardware was used because of its resistance to corrosion. All fasteners (nuts, bolts, screws, and threaded rod) were 304 (18-8) stainless steel. The 4-40 threaded rod used to attach the LVDT cores to the apparatus was 303 stainless steel.

METHODS

Data were analyzed using Matlab 6.5 R13, a numerical mathematics package

RESULTS AND DISCUSSION

Data Analysis

As of November 2003, some specimens had been exposed for more than a year and sufficient data were available to begin our analysis, which turned out to be far more complex than we had imagined when we began the experiment. Many of the experimental parameters did not fit our preconceived ideas. The data were analyzed in the following ways:

- (1) Daily cycles
- (2) Seasonal variations
 - Temperature
 - Relative humidity

- Maximum/minimum stress
 - Maximum/minimum strain
- (3) Tests for significance
 - (4) Elastic modulus

Daily Cycles

In a typical laboratory fatigue-cycle test, a mean stress, amplitude, and frequency are prescribed, and the material is cycled to failure. In outdoor tests, the cycles are not characterized as easily. We expected to observe diurnal cycles superimposed on a seasonal cycle. We did observe diurnal cycles, as shown in Figure 4. Several consecutive days are shown, but the cycles were quite different for each day. In this case, the daily change in moisture content was superimposed on drying over several days. The specimens were subjected to a cycle, but at a decreasing load and deflection on each of these days. When the wood became wetter over several days, load/deflection increased with each daily cycle.

In many cases, the cycle was further complicated by the lack of a clear diurnal cycle (Figure 5). Several mini-cycles or loops occurred on the day shown in Figure 5. We are fairly certain that this was caused by temperature-induced stress on days with intermittent cloud cover.

We want to be able to quantify the frequency and magnitude of cyclic motion experienced by each specimen. However, there are a number of problems with a "cycle" as the unit of motion. During a single interval, we observe a multiple changes in the strain direction that create strain loops of several sizes. We are currently working on develop a programmatic definition of "cycle" that captures loops of a certain size or larger. Once this is in place, we will be able to examine the distribution of loop sizes. With these data, we will develop a meaningful definition of cycle that can be used to evaluate cyclic fatigue. If cycles to failure are important, we will have a measure of the number of cycles. Knowing the cycles to failure will be necessary as we develop accelerated indoortests.

Seasonal Variation

One problem in testing that we have encountered with the TS and CS designs thus far has been centering specimens at installation. The specimens should have approximately the same amount of tension and compression in the extreme conditions during a year. We need to know the midpoint moisture content between the seasonal moisture content extremes. Therefore; we measure the seasonal cycles that the wood engines experience. The yearly

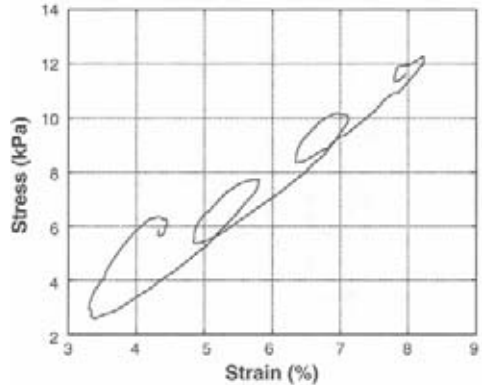


Figure 4-Stress/strain on sealant specimen, diurnal cycles over four days.

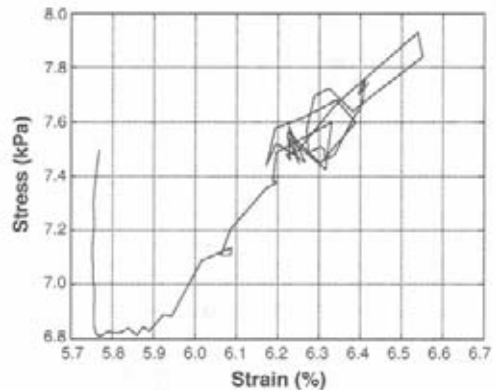


Figure 5-Stress/strain on sealant, loops during a single day.

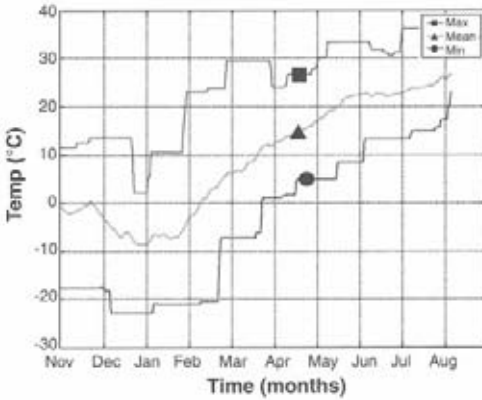


Figure 6-Seasonal maximum, minimum, and mean temperature variation in Madison, WI.

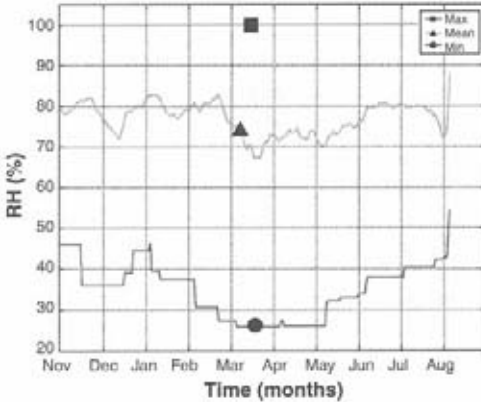


Figure 7-Seasonal maximum, minimum, and mean relative humidity (RH) variation in Madison, WI.

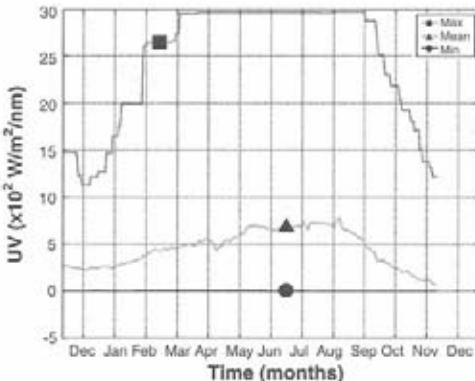


Figure 8 – UV spectral irradiance of 323.45 nm.

fluctuation in temperature, relative humidity, and UV radiation measured at the outdoor exposure site near Madison, WI, is shown in Figures 6–8.

Figure 6 shows the weekly maximum; minimum, and running seven-day mean temperatures experienced during the exposure. A similar plot for relative humidity is shown in Figure 7. It is interesting that RH always reached 100% at least once each week, probably during the night when the temperature was at the dew point. Figure 8 is a similar plot for UV radiation intensity. The UV irradiance for a year is shown in Figure 9. The peak height shows the total irradiance at 323.45 nm for each week.

Figure 10 shows the effects of relative humidity on the strain of one particular specimen, Q19. Strain was caused by the combined effect of temperature, RH, sunlight, and precipitatin—all of which caused the wood engine to change dimension. We can use data like this to determine the times of the year that cause high strain. Note that even though relative humidity was generally lower in April (Figure 7), the specimens experienced a high degree of movement during that month as a result of rain (Figure 10).

Figure 11 shows the effects of RH on the stress of specimen Q19. This specimen was selected at random for illustrative purposes. All the specimens followed curves of the same shape. Within the Q family, the data were all very similar. From measurement of this type we can determine the weathering dose: thermal histoy, wet/dry cycles, fatigue cycles, and total UV irradiance for any of the 18 UV wavelengths.

Tests for Significance

Before beginning an exhaustive analysis of our data, we decided to apply some statistical tests to ensure that the data were nonrandom. For this purpose,

we used a statistical tool called a normal value plot (NVP).⁹ An NVP plot measures data against a normal random distribution that has been scaled to match the extremes of the data. If the NVP shows a straight line at 45°, then the data are statistically random.

Fortunately, none of our data was found to be entirely random. Figure 12 shows an NVP for the strain data from one specimen. We added a line at 45° for reference. From this figure, we can gather that the strain on this specimen is statistically significant. We made similar plots for all our data, and all plots show the data to be significant.

Elastic Modulus

Our goal is to develop a cumulative damage model that will allow us to predict when sealants will fail. To do this, we need a measure of dose and a measure of performance. We developed dose measurements from the weather data. However, measurement of sealant performance is difficult. We decided to use the elastic modulus as one measure of performance. As already discussed, changes in this property can be an early indicator of failure. Elastic modulus (*E*) is defined as

$$E = \frac{\frac{\partial}{\partial t} \text{stress}}{\frac{\partial}{\partial t} \text{strain}}$$

There are also a number of conditions on *E*. It must be taken from a well-behaved loading cycle. The loading cycle must be executed at a constant strain rate. It must also be executed in a short enough time-scale that strain-relaxation and Mullin's recovery effects do not begin to take effect. Finally, this entire process must be completed at constant temperature.

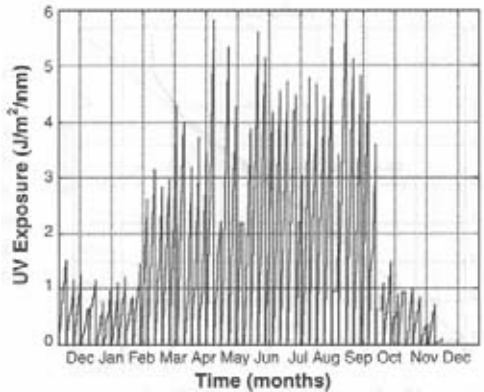


Figure 9-Weekly sums of spectral irradiance or 323.43 nm.

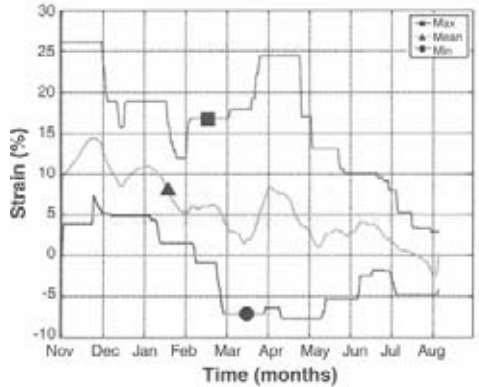


Figure 10-Maximum, minimum, and mean strain on specimen Q19.

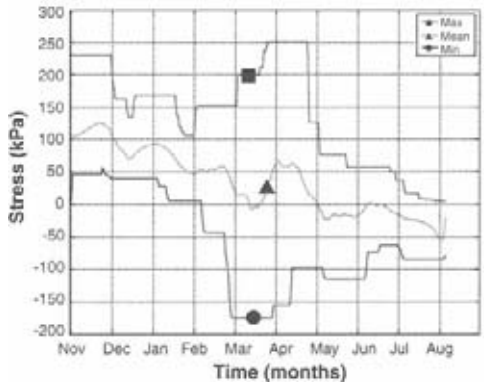
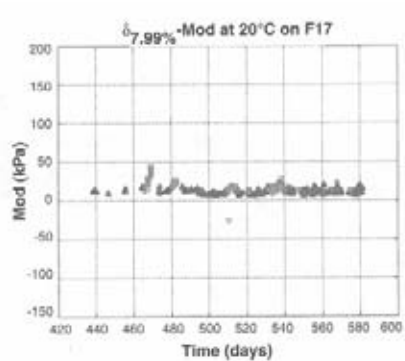
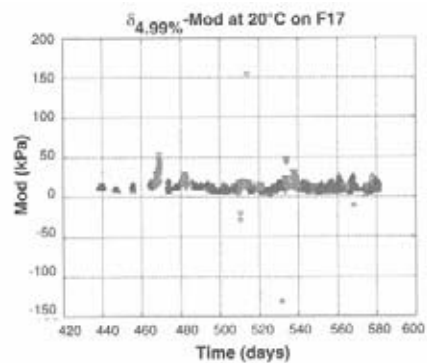
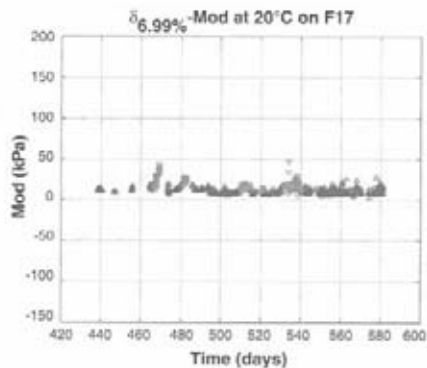
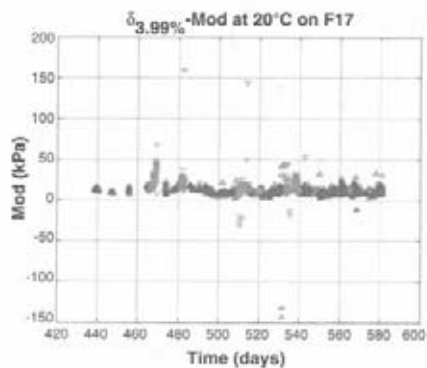
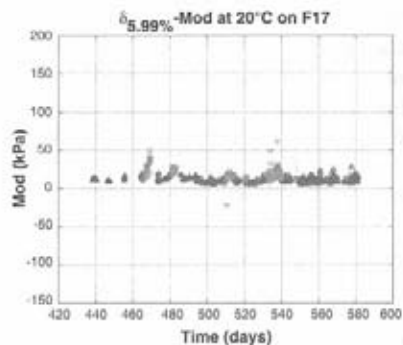
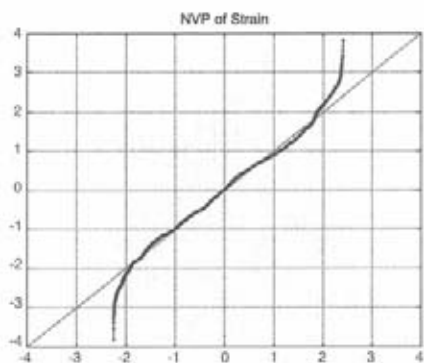


Figure 11-Maximum, minimum, and mean stress on specimen Q19.



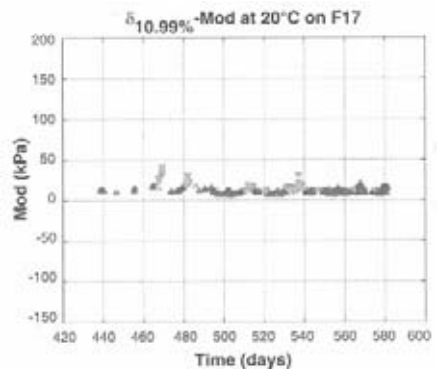
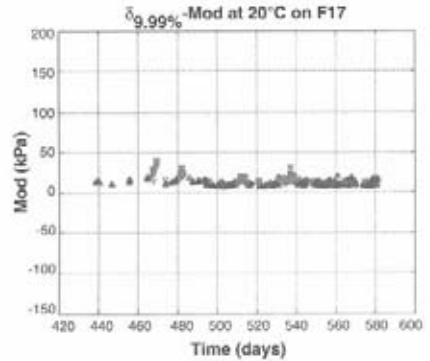
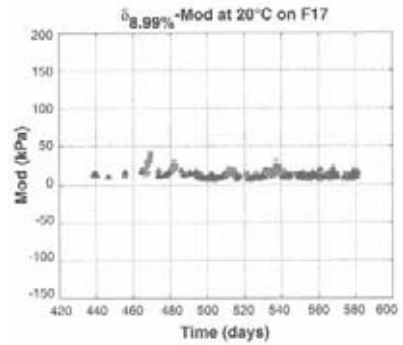
Unfortunately, the list of conditions for measuring E is one that we cannot obtain without more control of our experimental apparatus (i.e., control of the weather). Therefore, we have tried to find intervals in our data having constant and identical temperature, strain rate, and initial strain. *So far we have found that not a single condition causing a cycle has ever been repeated.* Therefore, we developed criteria for selecting data.

We are aware that initial stress and strain rates do play a role in the measurement of elastic modulus. However, their role seems to be smaller by some orders of magnitude than the role of temperature. We have the ability to select one exposure temperature and still have enough data with which to work. Therefore, we will be looking at data collected at constant temperature, in this case 20°C . We could have selected data at any temperature from -20°C to $+20^{\circ}\text{C}$.

We need to get approximations to the derivative of stress and strain in which we can place reasonable confidence. Without knowledge of the underlying functions that drive these systems, we cannot obtain the derivatives from discrete data. However, it is reasonable to assume that the driving functions are piecewise linear. Therefore, we can construct piecewise linear fits of the data to calculate the derivative.

We must consider two things in fitting the data. First, we must determine how many points to fit (i.e., “the width of the window”). Second, we must determine how tight a fit is required before we trust that it is an accurate model of what is really happening. We have found that fitting five points and requiring that the fit be tighter than $R^2 = 99\%$ delivers the best results. Wider windows or tighter fits do obtain fewer outlying points, but they also discard a large number of points that we consider acceptable.

The next series of figures show calculated values for the elastic modulus for a single specimen over approximately one year of



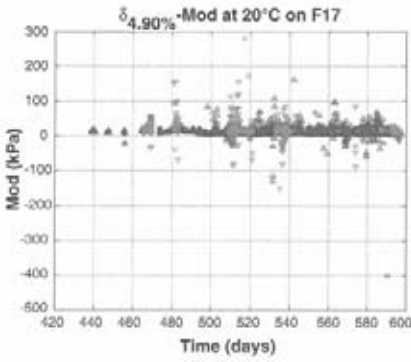


Figure 21-Modulus where $W = 4$, $R^2 > 90\%$.

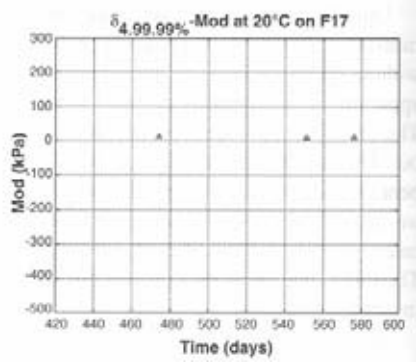


Figure 24-Modulus where $W = 4$, $R^2 > 99.99\%$.

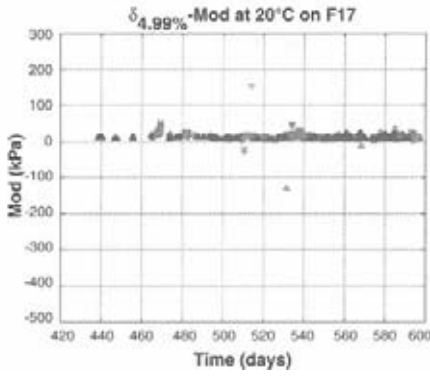


Figure 22-Modulus where $W = 4$, $R^2 > 99\%$.

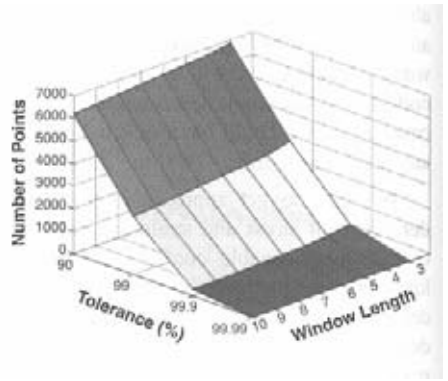


Figure 25-Combined effect of window length and R^2 filtering.

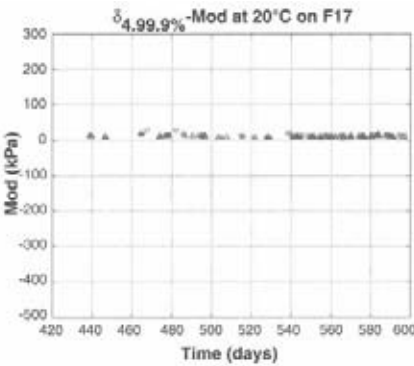


Figure 23-Modulus when $W = 4$, $R^2 = 99.9\%$

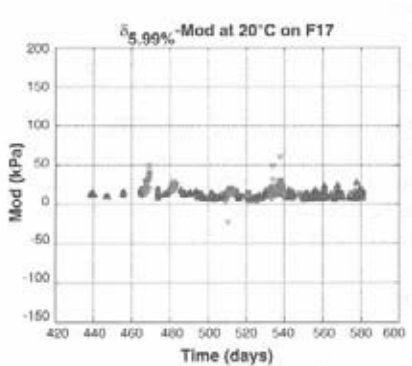


Figure 26-Approximation to elastic modulus.

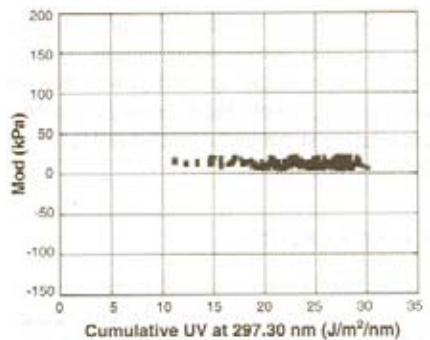
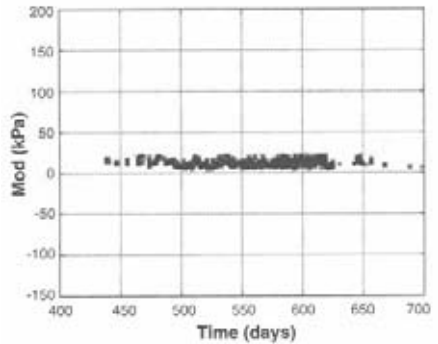
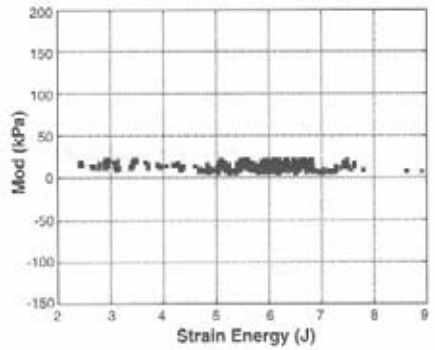
outdoor exposure. *Figures 13–20* show a series of plots for different window widths (3 to 10 points) for $R^2 = 99$. In the data, a triangle pointing up indicates tension and a triangle pointing down indicates compression. At a window width of three points (*Figure 13*), there are considerable data, but also a number of outliers. As the window width increases (*Figures 14–20*), the number of outliers decreases, but data are lost. At a window width of 10 points (*Figure 20*), there still appear to be outliers and few data remain.

The same evaluation can be done for the R^2 criteria. *Figures 21–24* show the data for a window width of 3 points and R^2 values of 90%, 99%, 99.9%, and 99.99%. As with window width, more rigorous selection decreases the number of outliers, but data are lost. At $R^2 = 99.99\%$ (*Figure 24*), only three points remain.

Figure 25 shows the combined effect of these two analyses. If one chooses a width of five points and $R^2 = 99\%$, about half the data remain in the data set. In this analysis, there is no attempt to choose a type of cycle. We selected responses at 20°C and have approximately 1,500 linear segments of five points with $R^2 = 99\%$. This analysis is for one specimen exposed outdoors for one year. Using the software we have developed, this same analysis can be done of all the specimens in just a few minutes.

Figure 26 shows our approximations to elastic modulus obtained using the 5.99% fitting method (i.e., window width of five points and confidence of 99%) plotted against time. It appears that the modulus did not change appreciably over the exposure interval for this specimen. This response could be plotted against other factors, e.g., number of cycles, total UV radiation, or any of the other weather factors in the database.

We are in the early stage of data analysis and the results presented here are preliminary. As we obtain data from the speci-



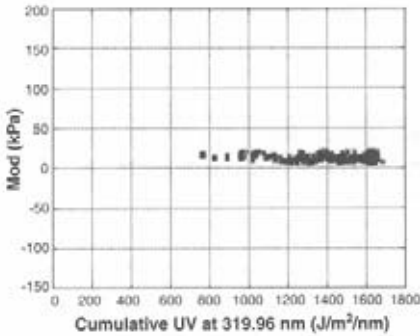


Figure 30-Modulus as function of UV exposure of 320 nm.

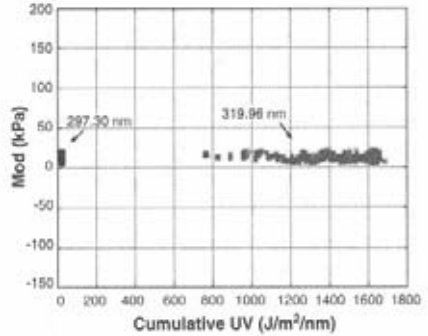


Figure 31-Modulus as function of cumulative UV exposure.

mens during colder weather, we will be able to compare elastic modulus at low temperatures over a year of outdoor exposure. Comparison at a low temperature should minimize some problems we are encountering with stress relaxation. If there has been a change in the crosslink density of the polymers, it should show up as a change in elastic modulus.

We have been examining a number of metrics for the dose experienced by a specimen. It makes no sense to plot our approximation to modulus against time, when time is not the factor that causes degradation. Unfortunately, some desirable metrics for dose (number of mechanical cycles, as one example) are as hard to obtain as is modulus itself. One dose metric that is simple to obtain is the cumulative strain energy of a specimen. The strain energy at time t is

$$\text{Abs}\{\text{force}(t)[\text{deflection}(t) - \text{deflection}(t-1)]\}$$

Qualitatively, this is the amount of mechanical work done on the specimen between time $t-1$ and time t . Cumulative strain energy is the sum of all the instantaneous strain energies. *Figure 27* shows modulus as a function of cumulative strain energy. For comparison, apparent modulus as a function of time is shown in *Figure 28*.

Another metric that is easy to obtain is the cumulative UV energy to which the specimens have been exposed. *Figures 29* and *30* present modulus as a function of UV exposure at two selected wave lengths. Note that the x -axis for these figures differs by some orders of magnitude. Note also that the shape and distribution of the data are different. This shows us that the UV exposure across wave lengths is not the same. This corresponds with what we would expect because the spectral power distribution decreases with decreasing wavelength. For comparison, we plotted *Figures 29* and *30* on the same scale in *Figure 31*. The analysis using cumulative strain and cumulative W exposure showed little change in this specimen during the exposure period.

CONCLUSIONS

We have demonstrated that the response of materials and the weather causing the response can be monitored continuously. The data can be analyzed to determine the elastic modulus of the material. If the modulus changes during exposure, this would indicate chemical change in the material. In addition, a small decrease in the load on the specimen could indicate loss of

adhesion to the substrate or cohesive failure of the sealant. The occurrence of these types of changes can be linked to the weather causing the degradation, and changes can be evaluated in terms of weather dose, not time of exposure.

References

- (1) *Annual Book of ASTM Standards*, Vol. 04.07, American Society for Testing and Materials, West Conshohocken, PA, 2000.
 C 718–93, Standard test method for ultraviolet (UV)–cold box exposure of one-part, elastomeric, solvent-release type sealants.
 C 719-98. Standard test method for adhesion and cohesion of elastomeric joint sealants under cyclic movement (Hockman cycle).
 C 732–95, Standard test method for aging effects of artificial weathering on latex sealants.
 C 734-93, Standard test method for low-temperature flexibility of latex sealants after artificial weathering.
 C 793–97, Standard test method for effects of accelerated weathering an elastomeric joint sealants.
 C 1257–94, Standard test method for accelerated weathering of solvent-release-type sealants.
 C 1442–99, Standard practice for conducting tests on sealants using artificial weathering apparatus.
 D 2249–94, Standard test method for predicting effect of weathering an face glazing and bedding compounds on metal sash.
- (2) Wolf, A.T., “Attempts at Correlating Accelerated Laboratory and Natural Outdoor Aging Results,” *Durability of Building Sealants*, Wolf, A.T. (Ed.), RILEM Pub., France, pp. 181–201, 1999.
- (3) Onuaha, U.O., “Durability of One-Part Polyurethane and Polyurethane-Hybrid Sealants,” *Durability of Building Sealants*, Wolf, A.T. (Ed.), RILEM Pub., France, pp. 235–251, 1999.
- (4) Brow, N.G., “Assessment of Joint Sealant by Outdoor Exposure in Cyclic Movement Testers,” Report No. 01.1.-2, CSIRO Division of Building Research, Highen, Victoria, Australia, pp. 16-22 (1965).
- (5) Burstrom, P.G., “Durability and Aging of Sealants,” *Durability of Building Materials and Components*, ASTM STP 691, Sereda, P.J. and Litvan, G.G. (Eds.), American Society for Testing and Materials, Philadelphia, PA, pp. 643-657, 1980.
- (6) Karpati, K.K., Solvason, M.R., and Senda, P.J., “Weathering Rack for Sealants,” *J. Coat. Technol.*, 49 (626) 44-47 (1977).
- (7) Lacasse, MA., “Advances in Test Methods to Assess the Long Term Performance of Sealants,” *Science and Technology of Building Seals, Seals, Sealants, Glazing and Waterproofing*, Myers, J.C. (Ed.), Vol. III, American Society for Testing and Materials, Philadelphia, PA, pp. 5–20, 1994.
- (8) Martin, J.W., “A Critical Review of the Role of Field-Exposure Experiments in Predicting the Service Life of Coatings,” *Plastics and Coatings–Durability, Stabilization, Testing*, Ryntz, R.A. (Ed.), Chapt. 2, Hanser Gardner Publications, Inc., Cincinnati, OH, p. 33, 2001.
- (9) DeVor, R.E., Chang, T.-H., and Sutherland, J.W., *Statistical Quality Design and Control*, Prentice Hall, Upper Saddle River, NY, pp. 90-94, 1992.

In: Martin, Jonathan W.; Ryntz, Rose A.; Dickie, Ray A. eds. Service Life Prediction: Challenging the Status Quo. Bluebell, PA: Federation of Societies of Coatings Technology: 171-185, 2005; Chapter 12. ISBN 0-934010-60-9.